HHS Public Access

Author manuscript

ACS Appl Nano Mater. Author manuscript; available in PMC 2019 September 28.

Published in final edited form as:

ACS Appl Nano Mater. 2018 September 28; 1(9): 4788–4800. doi:10.1021/acsanm.8b01000.

Adverse Interactions of Luminescent Semiconductor Quantum Dots with Liposomes and *Shewanella oneidensis*

Denise N. Williams[†], **Sunipa Pramanik**[‡], **Richard P. Brown**[†], **Bo Zhi**[‡], **Eileen McIntire**[‡], **Natalie V. Hudson-Smith**[‡], **Christy L. Haynes**[‡], and **Zeev Rosenzweig**[*,†]

[†]Department of Chemistry and Biochemistry, University of Maryland Baltimore County, Baltimore 21250, Maryland, United States

[‡]Department of Chemistry, University of Minnesota, Minneapolis 55455, Minnesota, United States

Abstract

Cadmium-containing luminescent quantum dots (QD) are increasingly used in display, bioimaging, and energy technologies; however, significant concerns have been raised about their potentially adverse impact on human health and the environment. This study makes use of a broad toolkit of analytical methods to investigate and increase our understanding of the interactions of luminescent cadmium-containing (CdSe) and cadmium-free (ZnSe) QD, with and without a passivating higher bandgap energy ZnS shell, with phospholipid vesicles (liposomes), which model bacterial membranes, and with *Shewanella oneidensis* MR-1, an environmentally relevant bacteria. A unique feature of this study is that all QD types have the same surface chemistry, being capped with uncharged poly(ethylene glycol) ligands. This enables focusing the study on the impact of the QD core on liposomes and bacterial cells. The study reveals that QD association with liposome and bacterial cell membranes is imperative for their adverse impact on liposomes and bacterial cells. The QD' concentration-dependent association with liposomes and bacterial cells destabilizes the membranes mechanically, which leads to membrane disruption and lysis in liposomes and to bacterial cell death. The study also shows that cadmium-containing QD exhibit a higher level of membrane disruption in bacterial cells than cadmium-free QD. ZnSe QD have low membrane impact, and coating them with a ZnS shell decreases their membrane disruption activity. In contrast, CdSe QD exhibit a high level of membrane impact, and coating them with a ZnS shell does not decrease, but in fact further increases, their membrane disruption activity. This behavior might be attributed to higher affinity and association of CdSe/ZnS QD with liposomes and bacterial cells and to a contribution of dissolved zinc ions from the ZnS shell to increased membrane disruption activity.

[*]**Corresponding Author:** zrosenzw@umbc.edu.

Author Contributions

The manuscript was written through contributions of all authors. All authors have given approval to the final version of the manuscript.

The authors declare no competing financial interest.

ASSOCIATED CONTENT

Supporting Information

The Supporting Information is available free of charge on the ACS Publications website at DOI: 10.1021/acsanm.8b01000.

TEM of QD, time-resolved photoluminescence measurements of QD, dynamic light scattering measurements of liposomes exposed to zinc and cadmium ion controls, viability results for *Shewanella oneidensis* MR-1 bacterial cells exposed to ZnSe and ZnSe/ZnS QD (DOCX)

Graphical Abstract

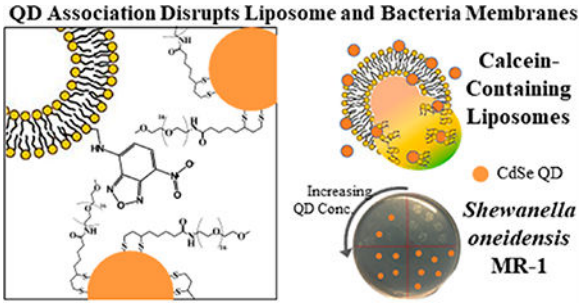

Keywords

quantum dots; liposomes; Shewanella oneidensis MR-1; membrane association; membrane disruption

INTRODUCTION

In the last two decades luminescent semiconductor quantum dots (QD) have been incorporated into a broad range of applications including bioimaging, solar cells, and display technologies.[1–7] Luminescent QD provide an attractive alternative to organic fluorophores in these applications because of their unique optical properties, including broad absorption peaks with high molar extinction coefficients, size-dependent narrow emission peaks, high emission quantum yield, and high chemical stability and photostability.[8] Historically, cadmium and lead-containing QD have been widely used because of their excellent photophysical properties and relatively simple syntheses.[1,9,10] However, concerns about the broad use of toxic metal-containing nanomaterials have limited large-scale development and use of QD technologies and led to efforts to replace cadmium and lead-containing QD with alternative nontoxic QD.[10–12] For example, ZnSe QD have been explored as a nontoxic alternative to CdS and CdSe QD.[7,13,14] This substitution comes with ease, since ZnSe QD are structurally similar and prepared using the same synthetic methodology as CdSe QD. This enables replacing cadmium with zinc in the QD cores while maintaining the same surface chemistry for all four QD types used in our study. Note that other optical nanomaterials, for example, InP,[15] graphene,[16] and silicon[17] QD have been explored as nontoxic alternatives to cadmium-containing QD in QD-based technologies, but variations in their surface chemistry make it difficult to compare their impact on liposomes and cells.[18]

Currently, a number of toxicity studies have demonstrated that ZnSe QD are less toxic than their cadmium-containing counterparts.[12,19] The adverse effects of cadmium-containing QD on cells and organisms were attributed to a combination of factors including the association of the QD with cell membranes, QD ion dissolution, and reactive oxygen species (ROS) generation (particularly when the QD are irradiated with a UV light), all factors with the capability to negatively impact model membranes and bacterial cells.[12,19] Several studies have found that coating cadmium-containing luminescent semiconductor QD with a passivating, higher-energy bandgap shell, decreases their toxicity toward cells and living organisms by inhibiting ROS generation and ion dissolution[15,20–22] Other studies revealed

that coating cadmium-containing QD with a passivating shell only delays adverse interactions of luminescent QD with cells and living organisms.[21,23–28] Cadmium dissolution is often described as a main contributor to QD toxicity.[21,28–30] In contrast, the role of zinc dissolution from commonly used CdSe/ZnS QD has not been considered as a main contributor to the toxicity of cadmium-containing QD, since the ZnS shell is often assumed to be inert.[25]

Our study describes the interactions between luminescent CdSe and ZnSe QD with phospholipid vesicles (liposomes), which model the membrane of Gram-negative bacteria, and with *Shewanella oneidensis* MR-1, an environmentally relevant Gram-negative bacterium, which is often used as a model organism for bioremediation research due to its metal-reducing capabilities.[31,32] ZnSe, ZnSe/ZnS, CdSe, and CdSe/ZnS QD were synthesized using nearly identical synthesis methods to ensure that the QD have the same surface chemistry and only differ in their cores. The synthesis, characterization, and careful control of surface chemistry of luminescent QD, rather than relying on commercially available QD with unknown surface content, is imperative to understand their interactions with model membranes and bacterial cells. Our study reveals that cadmium-containing QD have greater membrane disruption activity than cadmium-free QD, most likely due to increased membrane association and a higher rate of ion dissolution, which destabilize the liposome and bacterial cell membranes. Surprisingly, coating QD with a ZnS shell does not always decrease their membrane disruption activity. In CdSe/ZnS QD, structural irregularities, particularly when the QD are coated with a thick shell, lead to an increased dissolution rate of the ZnS shell. While zinc ion control measurements reveal that the liposomes are stable in the presence of zinc ions in the sample solutions, it is still possible that the increased rate of zinc ion dissolution adversely impacts the membrane of liposomes and bacterial cells when the CdSe/ZnS QD dissolve after they associate with the liposome or cell membranes.

MATERIALS AND METHODS

Reagents.

Zinc stearate (ZnSt), 1-dodecylphosphonic acid (DPA, 95%), zinc formate (98%), and zinc acetate were purchased from Alfa Aesar. 1-Octadecene (ODE), diphenyl phosphine (DPP), sulfur powder, trioctylphosphine (TOP, 97%), tetramethylammonium hydroxide solution (TMAH, 25 wt % in methanol), tetradecylphosphonic acid (97%), cadmium acetylacetonate (CdAcAc, 99.9%), sodium chloride, LUDOX TMA colloidal silica (34 wt % suspension in H_2O), and hexamethyldisilathiane ($(TMS)_2S$, synthesis grade) were purchased from Sigma-Aldrich. Selenium powder (Se, 99.5%), 1-hexadecylamine (HDA, 90%), oleylamine (C_{18} content 80–90%), and sodium hydroxide were purchased from Acros Organic. BD Difco Dehydrated Culture Media: Luria–Bertani (LB) broth, Dulbecco's Phosphate-Buffered Saline (without calcium and magnesium), BD Difco Dehydrated Culture Media: Granulated Agar, Corning Cellgro DPBS (1X), chloroform, toluene, methanol, 4-(2-hydroxyethyl)-1-piperazineethanesulfonic acid (HEPES) buffer (1 M), and nitric acid (Trace Metal grade) were purchased from Fisher Scientific. Instrument Calibration Standard 2 (5% HNO_3/ Tr. Tart. Acid/Tr. HF) for inductively coupled plasma mass spectrometry (ICP-MS) was

purchased from Claritas PPT SPEX CertiPrep. Dihydro Lipoic acidpolyethylene glycol (DHLA-PEG750-OCH_3) was prepared and purified with slight modifications to a previously reported protocol.[33,34] 1-palmitoyl-2-oleoyl-sn-glycero-3-phosphocholine (POPC), 1-palmitoyl-2-oleoyl-*sn*-glycero-3-phospho-(1′-rac-glycerol) (sodium salt) (POPG), and 1,2-dioleoyl-sn-glycero-3-phosphoethanolamine-N-(7-nitro-2–1,3-benzoxadiazol-4-yl) (ammonium salt) (NBD-POPE) were purchased from Avanti Polar Lipids, Inc. Calcein disodium salt (calcein) was purchased from Fluka. *S. oneidensis* MR-1 BAA-1096 was purchased from American Type Culture Collection.

ZnSe and ZnSe/ZnS QD Synthesis.

ZnSe and ZnSe/ZnS QD were synthesized according to a previously reported procedure.[14] The reaction was performed in a 25 mL three-neck round-bottom flask under stirring. The zinc precursor solution was prepared in the roundbottom flask by dissolving 632 mg (1 mmol) of ZnSt powder in 5.0 mL of ODE at 120 °C under inert nitrogen gas. The three-neck flask was under vacuum for 30 min and then backfilled with nitrogen gas while heating the solution to 280 °C. A selenium precursor solution was prepared by dissolving 7.9 mg of selenium powder in a solution containing 17 μL of DPP and 670 μL of toluene (selenium concentration of 0.15 M). This selenium solution was injected rapidly into the reaction mixture and allowed to react for 5 min at 280 °C before the flask was cooled to room temperature. A second selenium precursor solution was prepared by dissolving 78.9 mg of selenium powder in 800 μL of TOP (selenium concentration of 1.0 M). This selenium precursor solution was injected into the reaction mixture at room temperature. The reaction mixture was heated and kept at 280 °C for 20 min, then cooled to room temperature. The formed ZnSe QD were immediately coated with a ZnS shell or stored in their reaction mixture at room temperature and away from light. Two precursor solutions were prepared for the ZnS shelling: (1) 32.1 mg of sulfur powder in 1 mL of TOP (sulfur concentration of 1.0 M), and (2) 632 mg (1.0 mmol) of zinc stearate dissolved in 8 mL of ODE. The ZnS shell precursor solutions were injected into the reaction mixture at room temperature. The reaction mixture was then heated, kept at 280 °C for 20 min, and finally cooled to room temperature. The resulting ZnSe/ZnS QD were stored in the reaction mixture at room temperature and away from light. Prior to their immediate future use, QD were washed multiple times to remove excess reactants.

CdSe and CdSe/ZnS QD Synthesis.

CdSe QD were synthesized according to a previously reported procedure.[35] The reaction was performed in a 50 mL three-neck round-bottom flask under stirring. A cadmium precursor solution was prepared by dissolving 5.0 g of hexadecylamine in a 10 mL of TOP solution that also contained 2.1 mmol of tetradecylphosphonic acid and 1.0 mmol of CdAcAc. The solution was heated to 100 °C under inert nitrogen gas for the reactants to fully dissolve. The flask was under vacuum for 30 min and then backfilled with nitrogen gas. The solution was heated to 250 °C, cooled to 100 °C, and was under vacuum again for 30 min. After it was backfilled with nitrogen, the vessel was heated to 300 °C. A 5 mL selenium precursor solution, which contained 0.84 M selenium powder in TOP, was injected rapidly into the reaction mixture. The CdSe QD formed instantly, and the reaction mixture was cooled to 80 °C for overnight annealing. The resulting CdSe QD were stored in the

reaction mixture at room temperature and away from light. CdSe/ZnS QD were synthesized using successive ionic layer adsorption and reaction (SILAR). SILAR calculation and shelling was performed following a previously described protocol, where 0.3 nm radius monolayers of a ZnS shell are added one at a time.[36] Washed CdSe QD (0.15 μmol) were added to a solution that contained 6 mL of ODE, 4 mL of TOP, 6 mL of oleylamine, and 10 mg of dodecylphosphonic acid in a 50 mL round-bottom flask under nitrogen gas. The solution was heated and kept at 100 °C under high vacuum. The flask was backfilled with nitrogen gas. Then, the first aliquot of zinc precursor (0.05 M zinc formate in oleylamine), which was calculated from the core size to add a 0.3 nm radius monolayer of a ZnS shell, was injected over 15 min. The reaction mixture was heated and kept at 160 °C, and an aliquot of sulfur precursor (0.25 M $(TMS)_2S$ in TOP) was injected over 15 min to form the first monolayer of ZnS shell. The QD were then annealed at 160 °C for 20 min. The reaction mixture was heated and kept at 170 °C, while the process of adding zinc and sulfur precursors over 15 min and annealing over 20 min was repeated. The shelling process was repeated, each time at 10 °C higher temperature, until the desired ZnS shell thickness was realized. Finally, the reaction mixture was heated and kept at 200 °C, and 0.5 mL of oleic acid was added dropwise over 1 h. The reaction mixture was then allowed to slowly cool to room temperature.

Capping Luminescent QD with DHLA-PEG750-OCH3 Ligands.

Luminescent QD were capped with DHLA-PEG750-OCH_3 ligands (MW = 927 g/mol) to enable their aqueous solution miscibility. The ligand exchange process used to prepare the DHLA-PEG750-OCH_3 coated QD removed some Trioctylphosphine oxide (TOPO) ligands from the QD surface and shielded the remaining ones from interacting with liposome membranes and bacterial cells.[37] This is an imperative step to minimize the ligand contribution to QD toxicity, since TOPO ligands have been shown to be highly toxic.[38] The ligand exchange process was performed following a previously reported procedure.[39] The DHLA-PEG750-OCH_3 ligand (0.25 mmol), 0.5 mmol of sodium hydroxide, 0.13 mmol of zinc acetate, and 1 mL of methanol were sonicated together in a septum-closed vial filled under nitrogen gas. Purified QD (10 nmol) were dissolved with a minimal amount of chloroform, dried under vacuum, and put under a flow of nitrogen. The DHLA ligand solution was added to the QD solution and then left overnight at 50 °C under nitrogen gas. On the next day, 1 mL of ethyl acetate and enough hexane to separate the solvents into two distinct layers were added to the QD, stirred, and allowed to separate. The hexane layer was removed to waste. The QD in the ethyl acetate layer were dried under vacuum and then dispersed in Millipore water. The QD solution was passed through a 0.45 SFCA syringe filter into a 30 000 molecular weight cutoff (MWCO) spin filtration device for washing, using three centrifugation cycles at 2000g for 5 min at room temperature.

Absorbance and Fluorescence Instrumentation.

UV–Vis absorption spectra were obtained using a Thermo Scientific Evolution 201 UV–Vis spectrophotometer. Fluorescence spectroscopy measurements were performed using a PTI-Horiba QuantaMaster 400 fluorimeter, equipped with an integration sphere for emission quantum yield measurements, and with a PicoMaster TCSPC detector for fluorescence

lifetime measurements. A Molecular Devices SpectraMax M5 Microplate reader was used to measure changes in fluorescence emission over time.

Preparation of Calcein-Containing Liposomes.

10:1 molar POPC/POPG liposomes filled with calcein dye were prepared via a dehydration/rehydration method.[40] In a 500 mL round-bottom flask, 2 mL of 25 mg/mL POPC and 0.50 mL of 10 mg/mL POPG in chloroform were stirred together under nitrogen gas to create a dry phospholipid film. The flask was further vacuumed overnight to remove all organic solvent. A 5 mL stock solution containing 5 mM calcein disodium salt in 2 mM HEPES and 25 mM sodium chloride at pH 7.4 was prepared. An aliquot of 3 mL of the calcein solution was added to the dried lipids. The flask was immersed in dry ice–acetone bath, until the solid film began to dissociate from the bottom of the flask. The flask was then placed in a water bath at room temperature to form the liposomes. This process was repeated 10 times to ensure dye encapsulation in the liposomes. An aliquot of 1 mL of the liposome solution was extruded 15 times through an Avanti Polar Lipids 50 nm pore mini extruder with a polycarbonate membrane. The liposome sample was then run through a Sepharose CL-4B silica column (10 mm × 100 mm) with free HEPES buffer to remove free fluorophore molecules from the dye-containing liposomes.

Calcein-Containing Liposomes Lysis Assays.

Liposome lysis analysis used the time-based function of the PTI-Horiba QuantaMaster 400 fluorimeter. The excitation wavelength was set to 480 nm, the absorbance maximum of the dye. The emission of calcein was observed at 515 nm, until the fluorescence intensity stabilized typically after 15 min. The emission of leaked calcein after interactions with each test sample was observed for 20 min total, with stirring, at these parameters: 1–2 min to determine background fluorescence of liposomes, 15 min for substrate to interact with liposomes, 2–3 min for maximum liposome lysis to be determined after a 40 μL injection of 1% Triton X-100 in Millipore water.

Preparation of Dye-Free Liposomes.

10:1 molar POPC/POPG dye-free liposomes were prepared via the same methods, with the exception that phospholipids dried overnight were hydrated with 3 mL of 2 mM HEPES and 25 mM sodium chloride solution at pH 7.4, followed by dehydration/rehydration and extrusion.

Preparation of NBD-Labeled Liposomes.

10:1:0.1 molar POPC/POPG/NBD-POPE liposomes were prepared for an ~1% mol ratio of labeled to unlabeled lipids.[41] In a 250 mL round-bottom flask, 400 μL of 25 mg/mL POPC, 100 μL of 10 mg/mL POPG, and 100 μL of 10 mg/mL NBD-POPE in chloroform were stirred together under nitrogen gas to create a dry phospholipid film. The flask was further vacuumed overnight to remove all organic solvent. The next day, 7.5 mL of 2 mM HEPES and 25 mM sodium chloride at pH 7.4 was used to hydrate the lipids to a 2 mM lipid concentration. The flask was taken through 10 freeze/thaw cycles. Finally, 1 mL at a time,

the liposome solution was extruded 15 times through an Avanti Polar Lipids 50 nm pore mini extruder with a polycarbonate membrane.

Fluorescence Lifetime Assays of NBD-Labeled Liposomes

NBD-labeled liposome steady-state fluorescence was observed from 495 to 650 nm, with the excitation wavelength set to 470 nm. The fluorescence lifetime of NBD was observed at 515 nm.[42] Steady-state fluorescence and fluorescence lifetime measurements were conducted on the NBD-labeled liposomes alone, immediately after the addition of 0.5 nM QD, and at 4 h and 8 h following the addition of the QD to the samples. Only data collected at 4 h following the QD addition is shown.

Bacterial Culture and Colony Counting when Exposed to QD

Shewanella oneidensis MR-1 bacterial cells were cultured by streaking an LB-agar plate with bacterial cells and then incubating the plate in a 30 °C incubator overnight. Liquid cultures were grown by transferring colony inoculants from the plate to 10 mL of LB broth and incubating the bacterial cell suspensions for 4 h at 30 °C in an orbital shaker, to their mid log phase. Cells were then harvested by centrifugation for 10 min at 2000g, washed in Dulbecco's phosphate-buffered saline (D-PBS) buffer, and suspended in HEPES buffer solution (2 mM HEPES and 25 mM NaCl, at pH 7.4). The cultures were then diluted to 0.2 OD at 600 nm (OD600) to achieve a cell density of ~2×10^8 colony-forming units (CFUs) /mL. Serial 10-fold dilutions of this bacterial suspension were performed to achieve a cell concentration of 1×10^4 CFUs/mL in HEPES buffer. The resultant diluted bacterial suspension was treated with QD, in a total volume of 150 μL, at varying concentrations. The QD-exposed *Shewanella oneidensis*MR-1 bacterial cells were incubated on rotary shaker for 15 min, and then the viability of the cells was determined using a dropplate colony-counting protocol.[43] Six 10 μL droplets of the exposed bacterial suspensions and untreated negative controls were dropped on an LB-agar plate, which were presterilized under UV illumination for 20 min. The droplets were dried under air flow in a biological cabinet and then incubated at 30 °C for 20 h before colonies were counted using a Bantex Colony Counter 920A.

Inductively Coupled Plasma Mass Spectrometry of QD, QD Ion Dissolution, and QD Association with Bacterial Cells

Inductively coupled plasma mass spectrometry (ICP-MS) measurements of QD, bacterial cells, and QD-bacterial cell samples were performed using a PerkinElmer NexION 300D single quad mass spectrometer. The Instrument Calibration Standard 2 was used daily to prepare calibration curves from 0.1 ppb to 1 ppm for the different ion analytes (cadmium, selenium, zinc), which could be generated when the QD dissolve. Sample preparation for ICP-MS analysis was as follows: For QD in organic solvents, QD samples at predetermined concentrations, dissolved in chloroform, were put into scintillation vials containing acetone and centrifuged to precipitate out the QD. The QD were allowed to dry, nitric acid was added to dissolve the samples, and then Millipore water was added to the QD-nitric mixtures to dilute the nitric acid concentration to 2% by volume and a total sample volume of at least 5 mL. For QD in aqueous solution, QsD samples of predetermined concentrations were dissolved by adding nitric acid to the solutions. The solutions were kept at room temperature overnight. Millipore water was added to the QD-nitric acid mixtures to dilute the nitric acid

concentration to 2% by volume and a total sample volume of at least 5 mL. For investigation of QD dissolution, QD solutions of known concentrations were centrifuged through 30 000 MWCO spin filtration devices at 2000g, and the supernatants were analyzed for ion content. The level of association of QD with *Shewanella oneidensis* MR-1 bacterial cells was determined using ICP-MS measurements as follows: *Shewanella oneidensis* MR-1 bacterial cells were cultured in LB broth overnight. The resulting bacterial suspension was centrifuged for 10 min at 2000g, washed in D-PBS buffer, suspended in a HEPES buffer (2 mM HEPES and 25 mM NaCl, at pH 7.4), and the optical density (OD) was adjusted to 0.8 at 600 nm (OD600). The diluted bacterial suspension was treated with CdSe and CdSe/ZnS QD at concentrations equivalent to Cd core concentrations of 0.5, 1, and 2 mg/L. Similarly, the treatment concentrations used for the ZnSe and ZnSe/ZnS QD were equivalent to Zn core concentrations of 1, 2, and 5 mg/L. After an exposure time of 15 min, the bacterial cells were harvested as pellets by centrifugation at 2000g for 10 min. At this low speed of centrifugation only bacterial cells were precipitated along with associated QD, and free QD in the supernatant were discarded. The QD-treated bacterial cell pellets were analyzed using ICP-MS to determine the levels of cadmium and zinc, and to confirm QD association with bacterial cells.

Hyperspectral Imaging of CdSe and CdSe/ZnS QD and

Bacterial Cells. Images of *Shewanella oneidensis* MR-1 bacterial cells following incubation with CdSe or CdSe/ZnS QD were acquired using dark-field Cytoviva hyperspectral imaging (HSI; Cytoviva). In these experiments, sample solutions were drop-cast (~3–4 μL) onto a glass slide, which was then sealed with a coverslip and clear nail polish. Slides were examined at 100× magnification with an oil immersion lens under an Olympus BX-41 microscope. Spectral data were acquired with a Cytoviva spectrophotometer and integrated CCD camera in both the visible and near-infrared range (400–1000 nm). Analysis of the HSI spectra was performed by the Environment for Visualization software (ENVI 4.4 version). Spectral libraries of CdSe and CdSe/ZnS QD and *Shewanella oneidensis* MR-1 bacterial cells were used to help analyze HSI spectral angle mapper (SAM) spectral patterns and characterize association of the QD with bacterial cells.

High-Resolution Transmission Electron Microscopy of QD

High-resolution transmission electron microscopy (HR-TEM) images of QD were obtained using a Titan 80–300 S/TEM, operating at 300 kV with a Gatan OneView imaging camera. QD samples were drop-coated onto mesh copper grids with ultrathin carbon film on holey carbon support film (Ted Pella, Inc.). Grids were then placed in a vacuum oven overnight before analysis.

Biological Transmission Electron Microscopy of Bacterial Cells Incubated with QD

Biological transmission electron microscopy (BioTEM) images of *Shewanella oneidensis* MR1 bacterial cells exposed to QD were obtained using an FEI Tecnai T12 TEM after the following preparation. *Shewanella oneidensis* MR1 bacterial cells were cultured in LB broth overnight. The next day, the bacterial cells were washed with D-PBS buffer, diluted to an OD of 0.8 (OD600) in HEPES buffer at pH 7.4, then exposed to 1 mg/L of CdSe/ZnS QD for 15 min. This bacterial cell suspension was centrifuged down to a pellet, washed thrice

with 0.1 M cacodylate buffer solution, then resuspended in a fixation buffer of 2.5% glutaraldehyde in 0.1 M sodium cacodylate buffer and fixed for 50 min. The fixed bacterial cells were then centrifuged, washed with sodium cacodylate buffer, and dehydrated stepwise with increasing concentrations of ethanol (30, 50, 70, 80, 90, 95, and 100% ethanol in water). After the ethanol rinsing steps, the pellet was washed with propylene oxide three times. The resin infiltration steps were performed in the following manner. The pellet was soaked first in a 2:1 propylene oxide/epoxy resin mixture for 2 h and then in a 1:1 propylene oxide/epoxy resin mixture overnight. On text day, the 1:1 propylene oxide/epoxy resin mixture was removed and replaced with a fresh batch of 1:1 propylene oxide/epoxy resin mixture for 5 h, and finally incubated in a pure resin mixture and infiltrated overnight. The resin sample was then cured in a 40 °C oven for 1 d and then 60 °C oven for 2 d. Leica UC6 microtome and Diatome diamond knife were used to make ultrathin sections (65 nm) of this resin-embedded bacterial sample, and uranyl acetate and lead citrate were used to stain them. These sections were placed on copper TEM grids (Ted Pella Inc.).

RESULTS AND DISCUSSION

Characterization of Cadmium-Containing and Cadmium-Free QD.

Cadmium-containing CdSe and cadmium-free ZnSe QD were synthesized by the commonly used “hot injection” method.[14,35] The CdSe and ZnSe QD were coated with a ZnS shell following previously reported procedures.[14,36] UV–Vis absorption and emission spectra of CdSe and CdSe/ZnS QD are shown in Figure 1A. The UV–Vis absorption spectra show excitation peaks at 505 nm for CdSe QD and a red-shifted excitation peak at 552 nm for CdSe/ZnS QD. The emission spectra show corresponding emission peaks at 522 nm for CdSe QD and 580 nm for CdSe/ZnS QD. The emission quantum yields of CdSe and CdSe/ZnS QD were 13% and 43%, respectively. The full peak width at half-maximum (FWHM) of CdSe and CdSe/ZnS QD were 27 and 34 nm, respectively. The UV–Vis absorption and emission spectra of ZnSe and ZnSe/ZnS QD are shown in Figure 1B. The UV–Vis absorption spectra show excitation peaks at 410 and 418 nm for ZnSe and ZnSe/ZnS QD, respectively. The emission spectra show corresponding emission peaks at 418 for ZnSe QD and 423 nm for ZnSe/ZnS QD. The emission quantum yields of the ZnSe QD and ZnSe/ZnS QD were 5% and 10%, respectively. The FWHM of the ZnSe QD and ZnSe/ZnS QD were 17 and 15 nm, respectively. Time-resolved photoluminescence measurements were also performed to determine the impact of the ZnS shell on the cadmium-containing and cadmium-free QD (see Supporting Information for details). The fluorescence lifetime of CdSe QD was 29.6 ± 0.4 ns. It decreased to 16.9 ± 1.0 ns when the CdSe QD were coated with a ZnS shell to form CdSe/ZnS QD. The fluorescence lifetime of ZnSe QD was 7.4 ± 0.3 ns. It decreased to 6.4 ± 0.1 ns when the ZnSe QD were coated with a ZnS shell to form ZnSe/ZnS QD. This decrease in fluorescence lifetime when core QD are passivated with a higher-energy bandgap ZnS shell is attributed to increased confinement of the excited electrons in the core QD and is consistent with previous studies.[44] The distinct excitonic peaks in the UV–Vis spectra, the narrow and symmetric emission peaks, and the increase in emission quantum yield with a corresponding decrease in fluorescence lifetime when the QD are passivated with a higher energy bandgap shell suggest that both the cadmium-containing CdSe and CdSe/ZnS QD, and the cadmium-free ZnSe and ZnSe/ZnS

QD, are of high quality and display the photophysical properties required in luminescent QD based applications.

A ligand exchange reaction was performed to replace the organic capping ligands of the QD with uncharged DHLA-PEG750-OCH_3 ligands (Scheme 1). This allowed the QD to be dispersed in aqueous media and made them suitable for the liposome lysis and bacterial cell viability assays. More importantly, the use of the same capping ligand in all four QD types enabled direct comparison between the membrane disruption activity of cadmium-containing and cadmium-free QD.

Interactions of CdSe and ZnSe QD with Liposomes

Liposome lysis assays were performed to determine the membrane disruption activity of cadmium-containing CdSe and CdSe/ZnS QD and cadmium-free ZnSe and ZnSe/ZnS QD. Unlike bacteria or other living organisms, liposomes do not possess active mechanisms to degrade QD. Therefore, differences in the interactions between QD and liposome membrane could be attributed to differences in association of the QD with the liposome membrane due to differences in QD size, shape, and surface chemistry, and to differences in ion dissolution and ROS generation that could affect ion interactions with the liposome membrane. Note that the rates of ROS generation are negligible in our experiments, which are conducted under room light conditions in the absence of directed QD irradiation. Liposomes, with a phospholipid composition that models cell membranes of Gram-negative bacteria, were loaded with 10 mM calcein. Calcein was chosen as the fluorophore for the liposome lysis assays primarily because of its high encapsulation efficiency, and the high antileaking stability of calcein-containing liposomes in aqueous solutions.[45] Loading the liposomes with 10 mM calcein resulted in self-quenching of the fluorescent calcein molecules. The calcein-containing liposomes were exposed to increasing concentrations of cadmium-containing and cadmium-free QD up to 5 mg/mL selenium ion equivalents. The fluorescence of the calcein-containing liposomes was continuously measured at 515 nm (λ_{ex} = 480 nm) during the liposome lysis assays. Membrane disruption of the liposomes led to the release and dilution of calcein in the sample solutions, which in turn led to an increase in calcein fluorescence. The QD were selected to have minimal excitation at 470 nm and minimal fluorescence at 515 nm to minimize spectral overlap with calcein absorption and fluorescence.

Figure 2 describes the liposome lysis efficiency of the cadmium-containing and cadmium-free QD. Figure 2A shows the temporal dependence of calcein fluorescence (normalized) of the calcein-containing liposomes prior to QD exposure (background fluorescence), following the exposure of the liposomes to CdSe QD (black) and CdSe/ZnS QD (red), which contain 0.5 mg/L selenium ion equivalents in their core, and following the addition of 1% Triton solution to disrupt and release all the calcein molecules from the liposomes. The blue curve follows the fluorescence of calcein-free liposomes when CdSe/ZnS QD with 0.5 mg/L selenium ion equivalents in their core were added to the solution. The slight increase in fluorescence due to direct excitation of the CdSe/ZnS QD at 470 nm (an unfavorable excitation wavelength) represents the highest level of optical interference in our QD exposure experiments. The level of optical interference is significantly lower when CdSe, ZnSe and ZnSe/ZnS QD within the same concentration range are added to the calcein-free

liposome solutions. The contribution of QD emission due to direct excitation was therefore neglected based on these control measurements. Figure 2A,B shows that all QD types have membrane disruption activity. Figure 2A shows that CdSe/ZnS QD cause higher liposome lysis compared to non-shelled CdSe QD, which might be attributed to shell instability. In contrast, Figure 2B shows that ZnSe/ZnS QD cause less liposome lysis than nonshelled ZnSe QD, indicating a significantly higher ZnS shell stability on ZnSe QD relative to CdSe QD.

The percent liposome lysis efficiency of CdSe and CdSe/ZnS QD (Figure 2C) and ZnSe and ZnSe/ZnS QD (Figure 2D) was calculated based on the following expression:

$$\%\text{lysis} = \left[\left(I_{\text{eq}} - I_{\text{b}}\right)/\left(I_{\text{tri}} - I_{\text{b}}\right)\right] \times 100 \quad (1)$$

where I_{eq} is the fluorescence intensity of the liposomes when reaching equilibrium following the exposure of the calceincontaining liposomes to QD; I_b is the background fluorescence of the calcein-containing liposomes prior to QD exposure; and I_{tri} is the fluorescence intensity of the liposome sample following complete disruption and release of calcein molecules due to the exposure of the calcein-containing liposomes to the 1% Triton solution. Figure 2C,D shows the concentration dependence of the liposome lysis efficiency when the calcein-containing liposomes were exposed to increasing concentrations of CdSe QD and CdSe/ZnS QD (Figure 2C) and ZnSe and ZnSe/ZnS QD (Figure 2D). The membrane disruption activity is concentration-dependent for all QD types. Cadmium-containing CdSe and CdSe/ZnS QD exhibit higher levels of membrane disruption activity than cadmium-free ZnSe and ZnSe/ZnS QD. For example, exposure of the calcein-containing liposomes to CdSe and CdSe/ZnS QD with 0.5 mg/L selenium ion equivalents in their core resulted in 38 ± 1% and 42 ± 1% liposome lysis efficiency. In contrast, exposure of the calcein-containing liposomes to ZnSe and ZnSe/ZnS QD at 10-fold higher selenium ion equivalents in their cores resulted in 15 ± 4% and 10 ± 1% liposome lysis efficiency, respectively. Coating ZnSe QD with a ZnS shell decreased their membrane disruption activity almost to the level of liposome lysis observed when the calcein-containing liposomes were exposed to the DHLA-PEG ligands at parts per billion levels (the levels anticipated if all ligand molecules would be desorbed from the QD surface). In contrast, coating CdSe QD with a ZnS shell slightly increased, rather than decreased, their membrane disruption activity. The differences in lysis efficiency between CdSe and ZnSe QD, and the opposite effect of coating them with a ZnS shell on their membrane disruption activity was unexpected, since the synthesis methods used to prepare the CdSe and ZnSe QD and their surface chemistry were nearly identical. The source of this unexpected result is explored in the following paragraphs.

Liposomes Lysis Assays of CdSe/ZnS QD with Varying Shell

Thickness. Having observed an increase in membrane disruption activity when CdSe QD are coated with a ZnS shell, we investigated how the shell thickness affects the liposome lysis efficiency of CdSe/ZnS QD. TEM measurements were used to confirm an increase in QD size when CdSe QD were coated with a ZnS shell of increasing thickness (see Supporting Information for details). Figure 3A shows the temporal dependence of the fluorescence of

calcein-containing liposomes prior to QD exposure (background fluorescence), following the exposure to CdSe QD (black) and CdSe/ZnS QD with a shell thickness of one monolayer (green), three monolayers (red), and six monolayers (blue). All experiments were conducted with CdSe and CdSe/ZnS QD that contained 0.5 mg/L selenium ion equivalents in their core as was determined by ICP-MS. Control experiments involving the addition of CdSe and CdSe/ZnS QD of the same concentration to liposome-free and calcein-free liposome solutions showed an instant but negligible increase in QD fluorescence under our illumination conditions (λ_{ex} = 480 nm, λ_{em} = 515 nm). The negligible contribution of QD fluorescence is expected, since QD concentrations in our liposome lysis experiments are 3 orders of magnitude lower than the concentration of calcein in the liposome solution following liposome lysis. The liposome lysis efficiencies were calculated from the curves in Figure 3A using eq 1 (see above) as 44 ± 3% for CdSe QD (no shell), 42 ± 1% for CdSe/ZnS QD with one monolayer, 49 ± 3% for CdSe/ZnS QD with three monolayers, and 70 ± 1% CdSe/ZnS QD with six monolayers of ZnS shell thickness. A slower membrane disruption efficiency is observed when the liposomes are exposed to CdSe/ZnS QD with one monolayer shell; a shell thickness that seems to delay but not to prevent the liposome lysis. Further increase in shell thickness results in increasing liposome lysis efficiency, most significantly when the CdSe QD are coated with a thick six-monolayer ZnS shell.

ICP-MS measurements of cadmium, zinc, and selenium ions were used to determine the chemical stability of ZnSe QD, ZnSe/ZnS QD, CdSe QD, and CdSe/ZnS QD with varying shell thickness and concentration. Figure 3B describes the results of ICP-MS measurements used to determine the level of ion dissolution in CdSe and CdSe/ZnS QD with varying ZnS shell thickness between one and six monolayers at increasing concentrations from 0 to 0.5 mg/L selenium ion equivalents in QD that were added to a HEPES buffer at pH 7.4. The QD were incubated in HEPES buffer at room temperature for various time intervals ranging from 15 min to 24 h. The QD were then filtered out by passing the QD solution through a 30 000 MWCO filter under slow speed centrifugation of 2000g at room temperature. The levels of cadmium and selenium in the supernatant for all QD were negligible. In contrast, CdSe/ZnS QD exhibited significant zinc ion dissolution over 24 h, which increased with CdSe/ZnS QD concentration and ZnS shell thickness. Note that it is difficult to quantify the amount of released zinc ions from the QD due to high native levels of zinc in aqueous samples and glassware.[46] Nevertheless, the QD concentration dependence and ZnS shell thickness dependence of zinc ions levels in the samples strongly suggest a significant level of zinc ion dissolution, in the milligram per liter range, from the CdSe/ZnS QD within the time scale of our liposome lysis assays. It is therefore fair to conclude that zinc ion dissolution increases the adverse impact of CdSe/ZnS QD on the liposome membranes beyond their impact due to membrane association and disruption. It is important to note that the luminescence properties of the CdSe/ZnS QD, including emission quantum yield and peak width, do not change during the 15 min long incubation and liposome lysis assays, which were conducted in HEPES buffer at pH 7.4 and room temperature as well. This is consistent with previous studies in our laboratory, which showed that a single monolayer of ZnS shell is sufficient to realize ~90% enhancement in luminescence properties of CdSe/ZnS QD, and the value of additional ZnS shell layers is more in delaying the degradation of the core CdSe QD.[44] It is interesting to note that ZnSe/ZnS QD exhibited

significantly higher shell stability, and the levels of zinc ions in the supernatants of incubated ZnSe/ZnS QD were negligible (not shown). This was observed even though CdSe and ZnSe QD were coated with the same ZnS shell using nearly identical shelling conditions. The increased ZnS shell stability on ZnSe QD could be attributed to a greater crystal plane matching in ZnSe/ZnS than in CdSe/ZnS QD.

Association of QD with Liposomes as a Key Contributor to Liposome Membrane Disruption.

The ICP-MS results described above showed negligible cadmium and selenium ion dissolution from CdSe QD during 15 min long incubation in liposome-free and liposome-containing HEPES buffer solutions at pH 7.4. In addition, ion control experiments revealed a lack of lysis activity when liposomes were incubated for 15 min with QD supernatants (no QD in the incubation mixture), and in cadmium and selenium ion solutions at concentrations resulting from total dissolution of CdSe with 0.5 mg/L selenium ion equivalents in their cores. And yet, a measurable difference between the membrane disruption activity of CdSe and ZnSe QD and an increase in the membrane disruption activity of CdSe/ZnS QD with increasing shell thickness were observed. On the basis of these results we hypothesized that QD association with the liposome membranes plays a major role in the membrane disruption activity of QD and that the association of QD with liposomes differs for different QD types. Association between the QD and the liposome destabilizes the liposome membranes mechanically. The instability of ZnS shell on CdSe/ZnS QD results in zinc ion dissolution when the QD degrade, and the increase in local ion concentration near the membrane could also contribute to membrane disruption. To validate this hypothesis, we prepared NBD-labeled liposomes and investigated their interactions with CdSe and ZnSeQD. NBD is an environmentally sensitive dye. Fluorescence increase and fluorescence lifetime decrease were reported with decreasing polarity of the NBD environment.[42] In contrast, a fluorescence decrease was reported when NBD molecules react with ROS.[41] Fluorescence spectra of NBD prior to and following exposure of NBD liposomes to CdSe and ZnSe QD are shown in Figure 4A,B. The fluorescence spectra of NBD liposomes (λ_{ex} = 470 nm and $\lambda_{em\ max}$ = 515 nm) prior to and following QD exposure are shown in black and red, respectively. The residual fluorescence spectra of CdSe and ZnSe QD at this unfavorable excitation wavelength are shown in blue. A six-fold increase in the fluorescence intensity of the NBD liposomes is observed following their exposure to CdSe (Figure 4A) and ZnSe (Figure 4B) QD. This is attributed to decreased polarity of the NBD environment due to the associating of the PEG-coated QD with the liposome membranes, which effectively shield the NBD headgroup from water molecules and ions in the buffer solution. The lack of fluorescence decrease following the incubation of QD with the liposomes strongly suggests that ROS are not formed and therefore not a significant contributor to membrane disruption under our experimental conditions (short exposure, no UV irradiation). Fluorescence lifetime measurements shown in Figure 4C for CdSe and Figure 4D for ZnSe QD provide additional indication that the QD associate with the liposome membranes. Table 1 summarizes the fluorescence lifetime and the exponential terms used to fit the fluorescence lifetime decay curves of NBD liposomes prior and following a 4 h long exposure to CdSe and ZnSe QD. Decreases in the fluorescence lifetime from 5.87 ± 0.23 nsec to 5.17 ± 0.03 nsec and to 5.23 ± 0.03 nsec when the NBD liposomes are incubated for 4 h with CdSe and

ZnSe QD, respectively, are observed. Additionally, the fluorescence lifetime decay curve of NBD liposomes prior to QD exposure is described by two exponential terms with $\tau 1 = 2.81$ nsec and $\tau 2 = 9.58$ nsec with almost equal weights of ~55 and 45%. These two terms are attributed to the NBD heterogeneous environment, which is equally affected by the hydrophobic backbone of the liposome membrane and the outer aqueous environment of the liposomes. A significantly increased monoexponential character is observed when the poly(ethylene glycol) (PEG)-coated QD interact with the liposome membrane. The fluorescence lifetime decay curves (red) are still described by two exponential terms, for CdSe QD $\tau 1 = 3.78$ nsec and $\tau 2 = 9.24$ nsec and for ZnSe QD $\tau 1 = 3.84$ nsec and $\tau 2 = 9.43$ nsec, but their weights change to ~72 and 28% in both QD types. The decrease in fluorescence lifetime and the increase in monoexponential character of the fluorescence lifetime decay curves are consistent with a decrease in the polarity of the NBD environment, which is attributed to association of the PEG-coated QD with the NBD-labeled liposomes. As expected, the change in NBD fluorescence and fluorescence lifetime does not depend on the QD core composition. It only depends on the surface chemistry of the QD, which is nearly identical for CdSe and ZnSe QD, as both QD types undergo a ligand exchange process to replace TOPO with DHLA-PEG molecules to enable aqueous miscibility of the QD. Association of the QD with the liposome membranes is critical to their membrane disruption activity.

The Impact of Cadmium-Free and Cadmium-Containing QD on *Shewanella oneidensis* MR-1 Bacterial Cells.

The liposome lysis assays showed membrane disruption activity of all QD types, which is attributed to QD-membrane association that leads to membrane disruption. In our liposome experiments, CdSe and CdSe/ZnS QD showed higher membrane disruption activity than ZnSe and ZnSe/ZnS QD. We hypothesized that the interactions between the QD and negatively charged bacterial cell membranes would be similar to the interactions of QD with negatively charged liposomes. To test this hypothesis, we investigated the interactions between cadmium-free ZnSe and ZnSe/ZnS QD, and cadmium-containing CdSe and CdSe/ZnS QD, and *Shewanella oneidensis* MR-1 bacterial cells. *Shewanella oneidensis* MR-1 was chosen for the study, because it is an environmentally relevant bacterium, which was previously used in similar nanoparticle exposure studies.[31,32] We utilized TEM, ICP-MS, and hyperspectral imaging measurements to investigate the interactions between QD and bacterial cells and then measured the impact of QD exposure on bacterial cell viability.

TEM measurements provide qualitative assessment of the interactions between QD and bacterial cells. Representative TEM images of bacterial cells that were exposed to CdSe/ZnS QD, (the most disruptive QD to bacterial cells at a level of 1 mg/L cadmium ion equivalents (are shown in Figure 5. The low magnification required to view the bacterial cells (scale bars of 0.2 to 1 μm) enables the observation of dark spots, possibly of QD aggregates associated with the cells but not individual QD, which are only ~5 nm in diameter. Images A and B show distorted cells with the release of cell organelles as well as disintegrated cell membranes. Dark spots, possibly of QD aggregates, are seen on or near cells in the TEM images. The images reveal significant damage to the cells due to the interaction with the QD, which is consistent with our QD-liposome lysis assays.

ICP-MS experiments of washed bacterial samples digested following their incubation with ZnSe, ZnSe/ZnS, CdSe, and CdSe/ZnS QD were used to determine the level of association of these QD with *Shewanella oneidensis* MR-1 cells. Control measurements of digested pellets of *Shewanella oneidensis* MR1 cells in the absence of QD show no detectable zinc or cadmium ions. Digested pellets of bacterial cells that were incubated with 0.5 to 5 mg/L QD in HEPES buffer solutions at pH 7.4 show levels of cadmium (cadmium-containing QD) and zinc (cadmium-free QD) that were significantly higher than the levels of these ions in control QD samples in the absence of bacterial cells. For example, the washing of 2 mg/L CdSe/ZnS QD control (no bacteria) had a measured cadmium level of 27 μg/L. In contrast, when bacterial cells were exposed to 2 mg/L CdSe/ZnS QD the level of cadmium pelleted with the bacteria was ~10-fold higher at 200 μg/L. Interestingly, the level of cadmium and zinc in QD-bacterial samples, which were exposed to CdSe/ZnS and ZnSe/ZnS QD was three-fold higher than the level of cadmium and zinc in QD-bacterial samples that were exposed to CdSe and ZnSe core QD. The higher affinity of CdSe/ZnS QD than the affinity of CdSe QD to bacterial cells is consistent with the liposome assays described earlier, but the higher affinity of ZnSe/ZnS QD than ZnSe QD to bacterial cells is not. This shows the limitations of using simple liposomes to model complex bacterial cells. The higher levels of cadmium and zinc in QD-incubated bacterial cells provide additional evidence for QD-bacteria association.

Hyperspectral dark field microscopy was also used to study the interactions between QD and bacterial cells. This technique provides the capability to identify and locate objects, for example, nanoparticles and cells, as long as they show unique optical reflectance signature.[47] The method is somewhat limited in the ability to locate nanoparticles in the field, because it is diffraction limited but still able to indicate colocalization of the nanoparticles with the much larger bacterial cells. The hyperspectral data cube acquisition, namely, hyperspectral "pushbroom" scanning, generates three-dimensional (3D) data that consist of two spatial (x,y) and one spectral (z) dimensions.[48] Hence, a hyperspectral image can be treated as a dark field image with the spectral information associated with each pixel of the image.[49] The workflow includes dark field imaging, hyperspectral data acquisition, spectral library construction, spectral library filtering, and finally, QD and bacterial cell mapping. Figure 6 exhibits the hyperspectral images (left column) of *Shewanella oneidensis* Mr-1 (named *S. oneidensis* in the figure), CdSe QD, and CdSe/ZnS QD, and corresponding spectral libraries (right column) obtained by the region-of-interest (ROI) tool that converts selected pixels into spectral libraries for subsequent QD and bacterial cell mapping in QD-incubated bacterial samples. Specifically, 499 pixels were collected to build the *S. oneidensis* library, 438 pixels to build the CdSe QD library, and 403 pixels to build the CdSe/ZnS QD library. Maximum (max), minimum (min), and mean reflectance intensity are described in library files, along with standard deviation (±Stdev), from which it can be qualitatively determined that the average reflectance intensity of bacteria is much lower than those of QD. In addition, spectral library function anchored with CytoViva software was performed to cross-compare the libraries of bacteria and QD. It turned out that there was no library filtered out for both cases, indicating the uniqueness of their spectral files. Moreover, QD libraries were loaded into the spectral angle mapper (SAM) function to map the location of QD in the hyperspectral images of CdSe and CdSe/ZnS QD. The SAM function provides a convenient

and automated mapping method, of which the algorithm differentiates the spectral libraries and provides information about the location and analogy of endmember pixels in an input image.[49,50] This information allows us to map precise QD location and false-color them red. For the next step, the presence of QD colocalized with *Shewanella oneidensis* MR-1 cells after exposure was investigated using hyperspectral microscopy, as displayed by Figure 7. The pixels representing QD are pseudocolored with red. In both exposure samples, it is observable that there is proximity between QD and bacteria cells. The proximity, and in many cases overlap, between the spectral signatures for bacterial cells and QD supports our conclusion from the liposome assays that the QD associate with the negatively charged membranes. This in turn leads to a high local ion concentration as the QD dissolve, and to membrane disruption. As a caveat, the diffraction limit binds this imaging technique, so even overlap of spectral signatures does not guarantee direct physical contact between the micron-scale bacteria (which can be resolved) and the nanoscale QD (which cannot be resolved).

Realizing the important role of membrane association on the interactions between QD and liposomes and bacterial cells, we conducted bacterial cell viability assays to determine the impact of QD association on *Shewanella oneidensis* MR-1.

Bacterial cell cultures were exposed to ZnSe, ZnSe/ZnS, CdSe, or CdSe/ZnS QD at concentrations ranging from 0.01 to 0.5 mg/L selenium ion equivalents in the QD cores. Figure 8A shows bacterial cell cultures following exposure to increasing concentrations ranging from 0 to 0.5 mg/L of ZnSe (left) and CdSe (right) QD. Exposure of *Shewanella voneidensis* MR-1 to ZnSe QD had negligible impact on their viability even at the highest concentration of 0.5 mg/L selenium ion equivalents. Similarly, ZnSe/ZnS QD exposure did not impact bacterial cell viability (Figure S6). In contrast, exposure of *Shewanella oneidensis* MR-1 cells to CdSe QD at 0.01 mg/L selenium ion equivalents led to almost total reduction in bacterial cell viability. In agreement with the liposome assays, an even greater effect was observed when the bacterial cells were exposed to similar levels of CdSe/ZnS QD. To evaluate the relevance of the liposome assays as a model for the bacterial response to QD exposure, we also investigated the impact of CdSe/ZnS QD with varying shell thickness on the viability of *Shewanella oneidensis* MR-1 cells. Figure 8B describes the bacterial cell viability (%) as a function of CdSe/ ZnS QD concentration (selenium ion equivalents) for CdSe QD (black) and CdSe/ZnS QD with shell thickness of one monolayer (green), three monolayers (red), and six monolayers (red). A concentration-dependent decrease in bacterial viability is shown for all cadmium-based QD, and a greater decrease in bacterial viability is observed for CdSe/ZnS QD with increasing ZnS shell thickness. These results are indicative of the complex nature of the interactions between luminescent QD and bacterial cells. On one hand, passivating CdSe QD with a higher energy bandgap shell of ZnS is known to decrease the rate of ROS generation when irradiated and lower their toxicity.[15,20–22] On the other hand, the chemical instability of the shell likely due to crystal plane mismatches along the core/shell interface,[51,52] particularly in complex aqueous solutions, increases their rate of zinc ion dissolution and increases QD toxicity against the *S. oneidensis* MR-1 bacterial cells.

SUMMARY AND CONCLUSIONS

This study assessed the interactions between cadmium-containing and cadmium-free luminescent QD with negatively charged liposomes, which are often used to model Gram-negative bacteria, and *Shewanella oneidensis* MR-1, an environmentally relevant Gram-negative bacterium. Fluorescence lysis assays of calcein-containing liposomes show that all QD types interact with the liposomes, but the level of interactions is higher for cadmium-containing QD, especially CdSe/ZnS QD. The results suggest that association of the QD with the liposome membrane leads to membrane disruption, which is mechanical in nature and depends on the QD concentration and their affinity to the liposome membranes. The short time scale of the liposome lysis assays precludes ion dissolution of free QD (not associated with the membrane) as a main contributor to liposome lysis. Additionally, since the liposomes are only irradiated with room light, the observed membrane disruption cannot be attributed to ROS generation. BioTEM, ICP-MS, and hyperspectral imaging measurements suggest that the QD also associate with the negatively charged membranes of *Shewanella oneidensis* MR-1 bacterial cells. As expected, cadmium-free ZnSe and ZnSe/ZnS QD minimally impact the viability of *Shewanella oneidensis* MR-1 cells. In contrast, a short incubation of only 15 min, of CdSe or CdSe/ZnS QD to bacterial cells results in a significant reduction in bacterial cell viability. Ion control experiments show that, when CdSe or CdSe/ZnS QD are completely dissolved in solution, the resulting ion levels are not sufficient to induce a devastating impact on the cells, and yet exposure of the cells to QD does. The QD's impact on liposomes and bacterial cells in this study is attributed to strong association between the QD and liposomes or bacterial cells, which does not cease after the cells are separated from unbound QD to end the exposure. Surprisingly, the impact of shelling CdSe QD with a ZnS shell, which is done to enhance the QD emission properties, to minimize ROS generation, and to prevent direct contact between the toxic cadmium-containing cores and the liposomes or bacterial cell membranes, increases rather than decreases membrane disruption in both the liposomes and bacterial cell cultures. These are unwelcome findings, since it is generally accepted that shelling cadmium core QD with a ZnS shell would lower QD toxicity due to a reduced rate of ROS generation. The increased membrane disruption of CdSe/ZnS QD compared to CdSe QD and with increasing shell thickness could be attributed to increased affinity and association between CdSe/ZnS QD and liposomes and bacterial cells. It is also possible that crystal plane mismatches between the core CdSe QD and the ZnS shell leads to inherent chemical instability of CdSe/ZnS QD, [51,52] and in turn to a high rate of zinc ion dissolution from the QD. The dissolution of the ZnS following association of the CdSe/ZnS QD further destabilizes the membrane. The high local concentration of zinc ions near the membrane could also enhance membrane disruption of liposomes and bacterial cells.

Supplementary Material

Refer to Web version on PubMed Central for supplementary material.

ACKNOWLEDGMENTS

Work investigating liposome and bacterial response to quantum dots was supported by the National Science Foundation Center for Chemical Innovation (CCI) program Award No. CHE-1503408 for the Center for Sustainable

Nanotechnology. Work involving bacterial TEM characterization was performed in the Characterization Facility at the Univ. of Minnesota, which receives partial support from the MRSEC program (DMR-1420013). D.N.W. quantum dot syntheses were supported by the National Science Foundation Award No. CHE-1506995, including an NSF AGEP graduate fellowship award under CHE-1506995. Supplemental fellowship support to D.N.W. and R.P.B. was provided by the National Institute of Health Training Grant No. NIH-T32-GM066706. The authors thank Dr. A. Myers of the National Institute for Standards and Technology (NIST) Center for Nanoscale Science and Technology for assistance with HRTEM imaging and F. Zhou at the Univ. of Minnesota for microtoming BioTEM samples.

REFERENCES

(1). Kamat P; Scholes G Quantum Dots Continue to Shine Brightly. J. Phys. Chem. Lett 2016, 7, 584–585. [PubMed: 26842359]

(2). Liang X; Grice J; Zhu Y; Liu D; Sanchez W; Li Z; Crawford D; LeCouteur D; Cogger V; Liu X; Xu Z; Roberts M Intravital Multiphoton Imaging of the Selective Uptake of WaterDispersible Quantum Dots into Sinusoidal Liver Cells. Small 2015, 11, 1711–1720. [PubMed: 25504510]

(3). Xu G; Zeng S; Zhang B; Swihart M; Yong K; Prasad P New Generation Cadmium-Free Quantum Dots for Biophotonics and Nanomedicine. Chem. Rev 2016, 116, 12234–12327. [PubMed: 27657177]

(4). Bimberg D Quantum Dots for Lasers, Amplifiers and Computing. J. Phys. D: Appl. Phys 2005, 38, 2055–2058.

(5). Zhao K; Pan Z; Zhong X Charge Recombination Control for High Efficiency Quantum Dot Sensitized Solar Cells. J. Phys. Chem. Lett 2016, 7, 406–417. [PubMed: 26758605]

(6). Bang J; Park J; Lee J; Won N; Nam J; Lim J; Chang B; Lee H; Chon B; Shin J; Park J; Choi J; Cho K; Park S; Joo T; Kim S ZnTe/ZnSe (Core/Shell) Type-II Quantum Dots: Their Optical and Photovoltaic Properties. Chem. Mater 2010, 22, 233–240.

(7). Ji W; Jing P; Xu W; Yuan X; Wang Y; Zhao J; Jen A High Color Purity ZnSe/ZnS Core/Shell Quantum Dot Based Blue Light Emitting Diodes with an Inverted Device Structure. Appl. Phys. Lett 2013, 103, 053106.

(8). Vasudevan D; Gaddam R; Trinchi A; Cole I Core-Shell Quantum Dots: Properties and Applications. J. Alloys Compd 2015, 636, 395–404.

(9). Reiss P; Protiere M; Li L Core/Shell Semiconductor Nanocrystals. Small 2009, 5, 154–168. [PubMed: 19153991]

(10). Protesescu L; Yakunin S; Bodnarchuk M; Krieg F; Caputo R; Hendon C; Yang R; Walsh A; Kovalenko M Nanocrystals of Cesium Lead Halide Perovskites (CsPbX3, X = Cl, Br, and I): Novel Optoelectronic Materials Showing Bright Emission with Wide Color Gamut. Nano Lett. 2015, 15, 3692–3696. [PubMed: 25633588]

(11). Liu W; Zhang Y; Ruan C; Wang D; Zhang T; Feng Y; Gao W; Yin J; Wang Y; Riley A; Hu M; Yu W ZnCuInS/ZnSe/ ZnS Quantum Dot-Based Downconversion Light-Emitting Diodes and Their Thermal Effect. J. Nanomater 2015, 2015.

(12). Fu P; Xia Q; Hwang H; Ray P; Yu H Mechanisms of Nanotoxicity: Generation of Reactive Oxygen Species. J. Food Drug Anal 2014, 22, 64–75. [PubMed: 24673904]

(13). Drobintseva AO; Matyushkin LB; Aleksandrova OA; Drobintsev PD; Kvetnoy IM; Mazing DS; Moshnikov VA; Polyakova VO; Musikhin SF Colloidal CdSe and ZnSe/Mn Quantum Dots: Their Cytotoxicity and Effects on Cell Morphology. St. Petersburg Polytechnical University. Journal: Physics and Mathematics 2015, 1, 272–277.

(14). Ippen C; Greco T; Kim Y; Kim J; Oh M; Han C; Wedel A ZnSe/ZnS Quantum Dots as Emitting Material in Blue QD-LEDs with Narrow Emission Peak and Wavelength Tunability. Org. Electron 2014, 15, 126–131.

(15). Xie R; Battaglia D; Peng X Colloidal InP Nanocrystals as Efficient Emitters Covering Blue to Near-Infrared. J. Am. Chem. Soc 2007, 129, 15432. [PubMed: 18034486]

(16). Zhao Y; Liu Q; Shakoor S; Gong J; Wang D Transgenerational Safety of Nitrogen-doped Graphene Quantum Dots and the Underlying Cellular Mechanism in Caenorhabditis elegans. Toxicol. Res 2015, 4, 270–280.

(17). Erogbogbo F; Yong K; Roy I; Xu G; Prasad P; Swihart M Biocompatible Luminescent Silicon Quantum Dots for Imaging of Cancer Cells. ACS Nano 2008, 2, 873–878. [PubMed: 19206483]

(18). Das A; Snee P Synthetic Developments of Nontoxic Quantum Dots. ChemPhysChem 2016, 17, 598–617. [PubMed: 26548450]

(19). Maurer-Jones M; Gunsolus I; Murphy C; Haynes C Toxicity of Engineered Nanoparticles in the Environment. Anal. Chem 2013, 85, 3036–3049. [PubMed: 23427995]

(20). Priester J; Stoimenov P; Mielke R; Webb S; Ehrhardt C; Zhang J; Stucky G; Holden P Effects of Soluble Cadmium Salts Versus CdSe Quantum Dots on the Growth of Planktonic Pseudomonas aeruginosa. Environ. Sci. Technol 2009, 43, 2589–2594. [PubMed: 19452921]

(21). Derfus A; Chan W; Bhatia S Probing the Cytotoxicity of Semiconductor Quantum Dots. Nano Lett. 2004, 4, 11–18. [PubMed: 28890669]

(22). Lai L; Li S; Feng J; Mei P; Ren Z; Chang Y; Liu Y Effects of Surface Charges on the Bactericide Activity of CdTe/ZnS Quantum Dots: A Cell Membrane Disruption Perspective. Langmuir 2017, 33, 2378–2386. [PubMed: 28178781]

(23). Lu Z; Li C; Bao H; Qiao Y; Toh Y; Yang X Mechanism of Antimicrobial Activity of CdTe Quantum Dots. Langmuir 2008, 24, 5445–5452. [PubMed: 18419147]

(24). Green M; Howman E Semiconductor Quantum Dots and Free Radical Induced DNA Nicking. Chem. Commun 2005, 0, 121–123.

(25). Manshian B; Soenen S; Al-Ali A; Brown A; Hondow N; Wills J; Jenkins G; Doak S Cell Type-Dependent Changes in CdSe/ZnS Quantum Dot Uptake and Toxic Endpoints. Toxicol. Sci 2015, 144, 246–258. [PubMed: 25601991]

(26). Hardman R A Toxicologic Review of Quantum Dots: Toxicity Depends on Physicochemical and Environmental Factors. Environ. Health Perspect 2006, 114, 165–172. [PubMed: 16451849]

(27). Yong K; Ding H; Roy I; Law W; Bergey E; Maitra A; Prasad P Imaging Pancreatic Cancer Using Bioconjugated InP Quantum Dots. ACS Nano 2009, 3, 502–510. [PubMed: 19243145]

(28). Mo D; Hu L; Zeng G; Chen G; Wan J; Yu Z; Huang Z; He K; Zhang C; Cheng M Cadmium-Containing Quantum Dots: Properties, Applications, and Toxicity. Appl. Microbiol. Biotechnol 2017, 101, 2713–2733. [PubMed: 28251268]

(29). Medintz I; Uyeda H; Goldman E; Mattoussi H Quantum Dot Bioconjugates for Imaging, Labelling and Sensing. Nat. Mater 2005, 4, 435–446. [PubMed: 15928695]

(30). Mahendra S; Zhu H; Colvin V; Alvarez P Quantum Dot Weathering Results in Microbial Toxicity. Environ. Sci. Technol 2008, 42, 9424–9430. [PubMed: 19174926]

(31). Heidelberg J; Paulsen I; Nelson K; Gaidos E; Nelson W; Read T; Eisen J; Seshadri R; Ward N; Methe B; Clayton R; Meyer T; Tsapin A; Scott J; Beanan M; Brinkac L; Daugherty S; DeBoy R; Dodson R; Durkin A; Haft D; Kolonay J; Madupu R; Peterson J; Umayam L; White O; Wolf A; Vamathevan J; Weidman J; Impraim M; Lee K; Berry K; Lee C; Mueller J; Khouri H; Gill J; Utterback T; McDonald L; Feldblyum T; Smith H; Venter J; Nealson K; Fraser C Genome Sequence of the Dissimilatory Metal Ion-Reducing Bacterium Shewanella oneidensis. Nat. Biotechnol 2002, 20, 1118–1123. [PubMed: 12368813]

(32). Hang M; Gunsolus I; Wayland H; Melby E; Mensch A; Hurley K; Pedersen J; Haynes C; Hamers R Impact of Nanoscale Lithium Nickel Manganese Cobalt Oxide (NMC) on the Bacterium Shewanella oneidensis MR-1. Chem. Mater 2016, 28, 1092–1100.

(33). Mei B; Susumu K; Medintz I; Mattoussi H Polyethylene Glycol-based Bidentate Ligands to Enhance Quantum Dot and Gold Nanoparticle Stability in Biological Media. Nat. Protoc 2009, 4, 412–423. [PubMed: 19265800]

(34). Mei B; Susumu K; Medintz I; Delehanty J; Mountziaris T; Mattoussi H Modular Poly(ethylene glycol) Ligands for Biocompatible Semiconductor and Gold Nanocrystals with Extended pH and Ionic Stability. J. Mater. Chem 2008, 18, 4949–4958.

(35). Jasieniak J; Smith L; van Embden J; Mulvaney P; Califano M Re-examination of the Size-Dependent Absorption Properties of CdSe Quantum Dots. J. Phys. Chem. C 2009, 113 (45), 19468–19474.

(36). Xie R; Kolb U; Li J; Basche T; Mews A Synthesis and Characterization of Highly Luminescent CdSe-Core CdS/ Zn0.5Cd0.5S/ZnS multishell nanocrystals. J. Am. Chem. Soc 2005, 127, 7480–7488. [PubMed: 15898798]

(37). Wenger W; Bates F; Aydil E Functionalization of Cadmium Selenide Quantum Dots with Poly(ethylene glycol): Ligand Exchange, Surface Coverage, and Dispersion Stability. Langmuir 2017, 33, 8239–8245. [PubMed: 28768415]

(38). Zhang L; Shen X; Liang H; Chen F; Huang H Phosphinefree synthesis of ZnSe:Mn and ZnSe:Mn/ZnS doped quantum dots using new Se and S precursors. New J. Chem 2014, 38, 448–454.

(39). Liu D; Snee P Water-Soluble Semiconductor Nanocrystals Cap Exchanged with Metalated Ligands. ACS Nano 2011, 5, 546–550. [PubMed: 21141814]

(40). Zheng Z; Saar J; Zhi B; Gallagher MJ; Fairbrother DH; Haynes CL; Lienkamp K; Rosenzweig Z Structure-Property Relationships of Amine-Rich and Membrane-Disruptive Poly(oxonorbornene)-Coated Gold Nanoparticles. Langmuir 2018, 34, 4614–4625. [PubMed: 29558808]

(41). Fortier C Preparation, Characterization, And Application of Liposomes in the Study of Lipid Oxidation Targeting Hydroxyl Radicals. Ph.D. Dissertation, University of New Orleans, 2008.

(42). Haldar S; Chattopadhyay A Application of NBD-labeled Lipids in Membrane and Cell Biology In Fluorescent Methods to Study Biological Membranes; Springer: Berlin, Germany, 2012; Vol. 13.

(43). Feng Z; Gunsolus I; Qiu T; Hurley K; Nyberg L; Frew H; Johnson K; Vartanian A; Jacob L; Lohse S; Torelli M; Hamers R; Murphy C; Haynes C Impacts of Gold Nanoparticle Charge and Ligand Type on Surface Binding and Toxicity to Gram-negative and Gram-positive Bacteria. Chem. Sci 2015, 6, 5186–5196. [PubMed: 29449924]

(44). Lyons T; Williams D; Rosenzweig Z Addition of Fluorescence Lifetime Spectroscopy to the Tool Kit Used to Study the Formation and Degradation of Luminescent Quantum Dots in Solution. Langmuir 2017, 33, 3018–3027. [PubMed: 28245133]

(45). Were L; Bruce B; Davidson P; Weiss J Size, Stability, and Entrapment Efficiency of Phospholipid Nanocapsules Containing Polypeptide Antimicrobials. J. Agric. Food Chem 2003, 51, 8073–8079. [PubMed: 14690399]

(46). Cornelison G; Mihic S Contaminating Levels of Zinc Found in Commonly-used Labware and Buffers Affect Glycine Receptor Currents. Brain Res. Bull 2014, 100, 1–5. [PubMed: 24177173]

(47). Verebes GS; Melchiorre M; Garcia-Leis A; Ferreri C; Marzetti C; Torreggiani A Hyperspectral Enhanced Dark Field Microscopy for Imaging Blood Cells. J. Biophotonics 2013, 6, 960–967. [PubMed: 23913514]

(48). Gao L; Smith RT Optical Hyperspectral Imaging in Microscopy and Spectroscopy–A Review of Data Acquisition. J. Biophotonics 2015, 8, 441–456. [PubMed: 25186815]

(49). Zamora-Perez P; Tsoutsi D; Xu R; Rivera-Gil P Hyperspectral-Enhanced Dark Field Microscopy for Single and Collective Nanoparticle Characterization in Biological Environments. Materials 2018, 11, 243.

(50). Peña MDPS; Gottipati A; Tahiliani S; Neu-Baker NM; Frame MD; Friedman AJ; Brenner SA Hyperspectral Imaging of Nanoparticles in Biological Samples: Simultaneous Visualization and Elemental Identification. Microsc. Res. Tech 2016, 79, 349–358. [PubMed: 26864497]

(51). Gong K; Kelley D A Predictive Model of Shell Morphology in CdSe/CdS Core/Shell Quantum Dots. J. Chem. Phys 2014, 141, 194704. [PubMed: 25416902]

(52). Yu Z; Guo L; Du H; Krauss T; Silcox J Shell Distribution on Colloidal CdSe/ZnS Quantum Dosts. Nano Lett. 2005, 5, 565–570. [PubMed: 15826088]

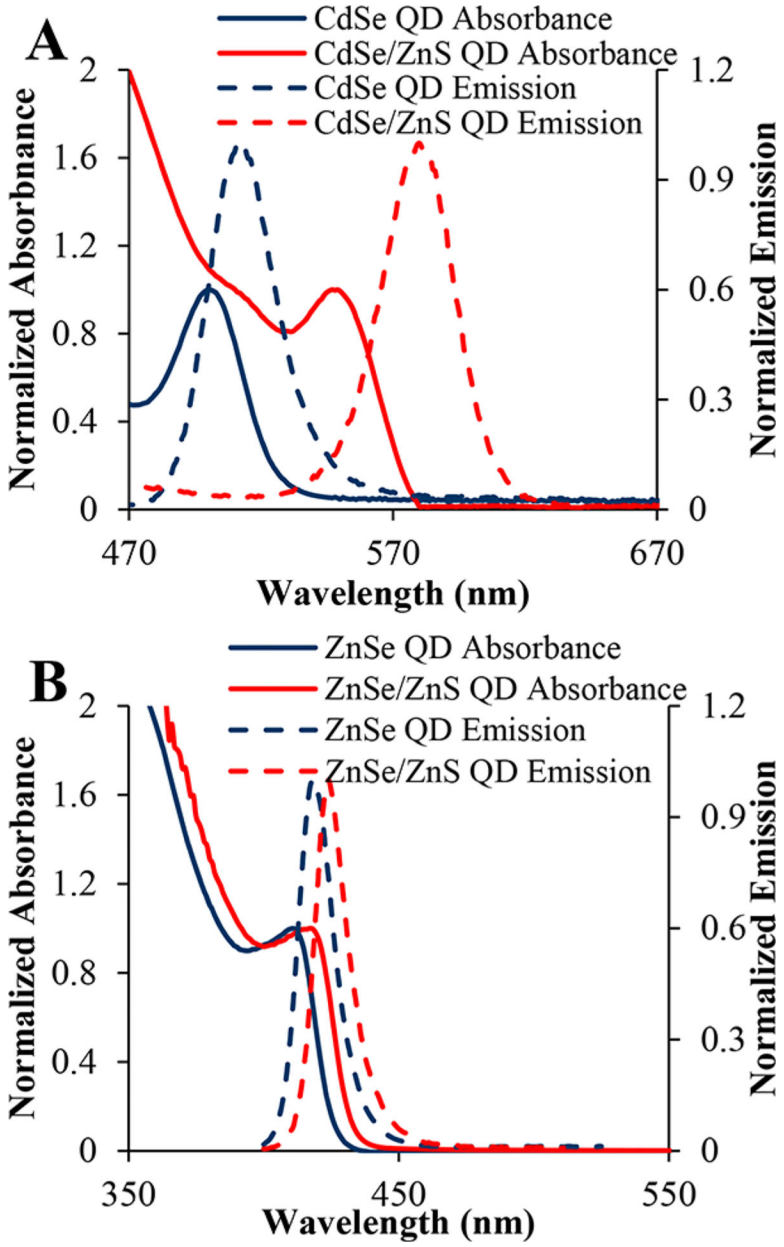

Figure 1.

Normalized absorbance and emission spectra of CdSe and CdSe/ZnS QD (λ_{ex} = 375 nm) (A) and ZnSe and ZnSe/ZnS QD (λ_{ex} = 350 nm) (B).

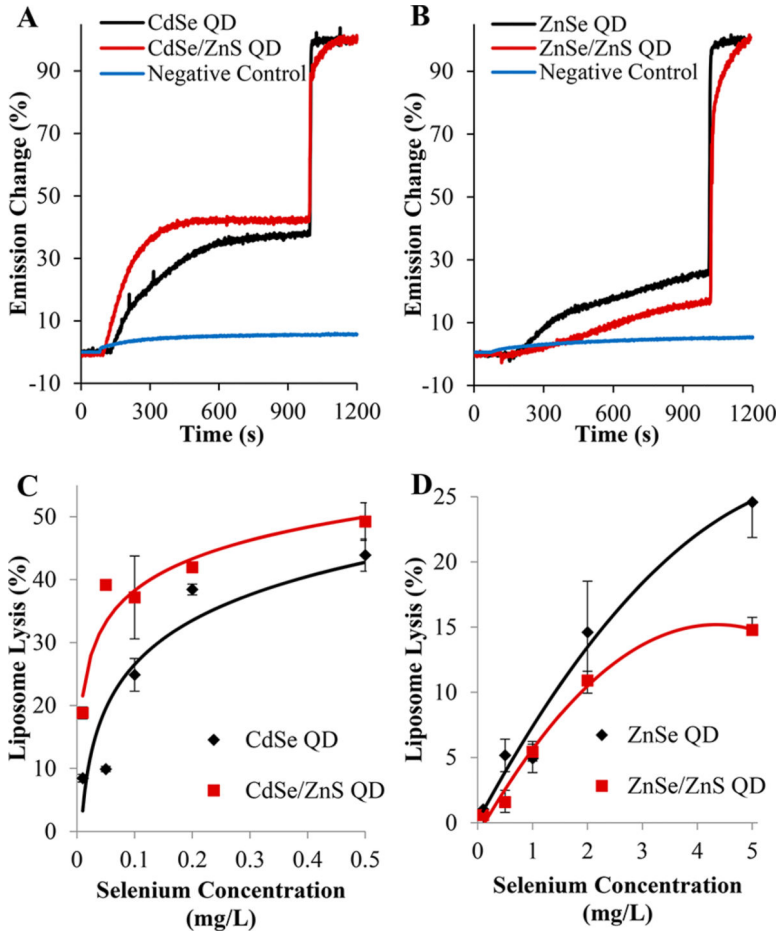

Figure 2.

Normalized emission traces comparing the membrane disruption activity of CdSe and CdSe/ZnS QD (A) and ZnSe and ZnSe/ZnS QD (B). The negative control (blue) curves follow the exposure of calcein-free liposomes to CdSe/ZnS QD (A) and ZnSe/ ZnS QD (B). (C) The concentration dependence of the liposome lysis efficiency for CdSe (black) and CdSe/ZnS (red) QD. (D) The concentration dependence of the lysis efficiency for ZnSe (black) and ZnSe/ZnS (red) QD. Each liposome lysis efficiency value is the average of three replicate measurements ($N = 3$). The error bars are ± standard deviation from the mean value.

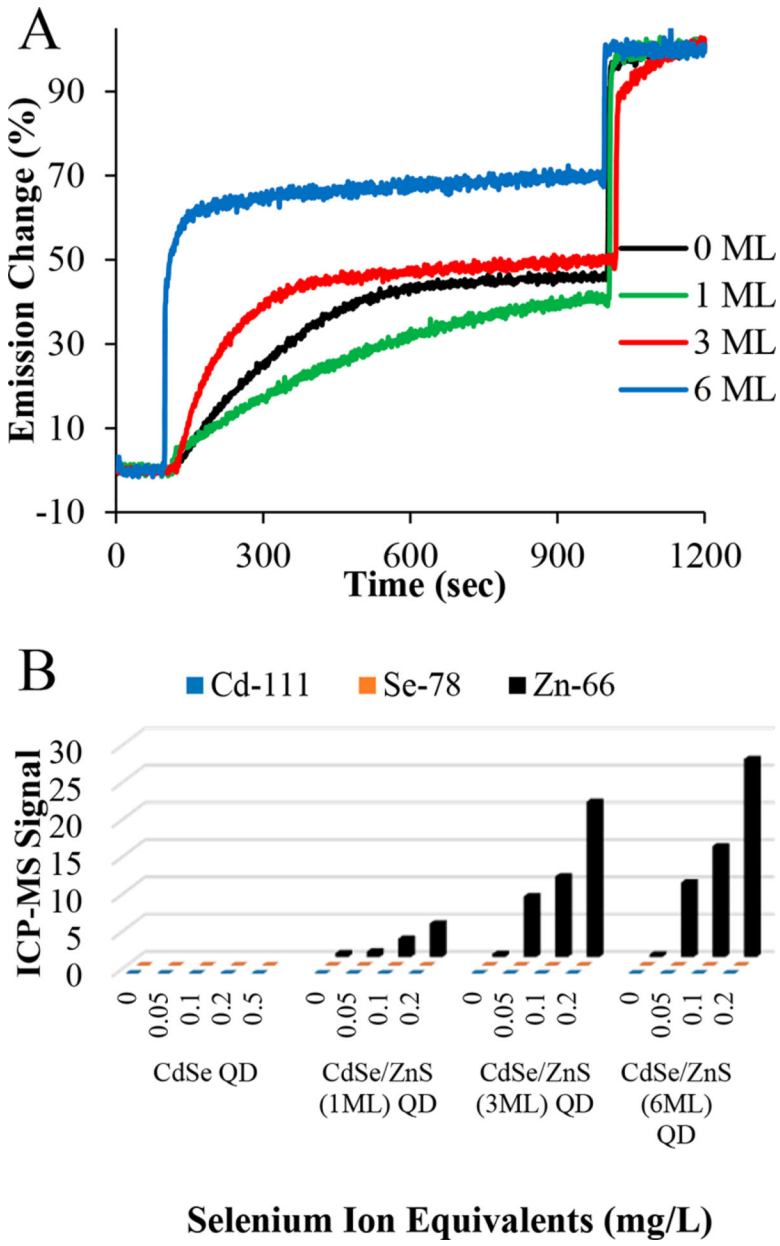

Figure 3.

Normalized emission traces from calcein-filled liposomes when exposed to CdSe QD with 0 to 6 monolayers (ML) (A). ICP-MS signal intensities of zinc, cadmium, and selenium ions resulting from the dissolution of CdSe QD and CdSe/ZnS QD with one, three, and six monolayers shell in HEPES buffer at pH 7.4 (B). Only zinc ion dissolution is observed indicating degradation of the ZnS shell. $N = 3$ for each condition, and error bars are omitted for clarity.

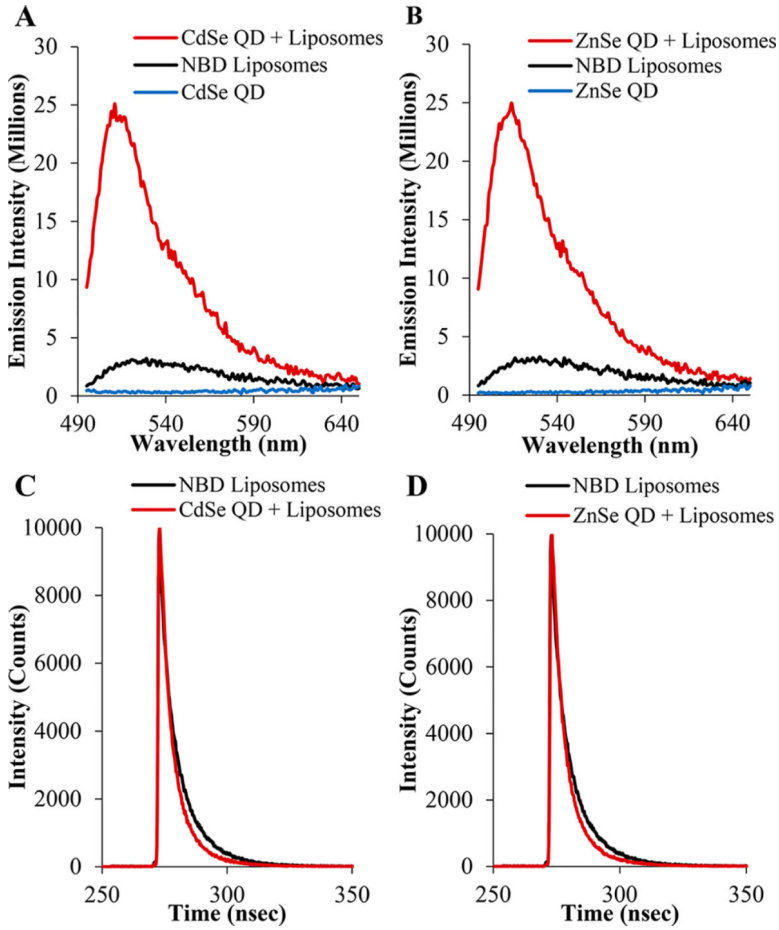

Figure 4.

Fluorescence intensity of NBD-labeled liposomes (black), QD (blue), and following a 4 h incubation of NBD-labeled liposomes with QD (red) show significant NBD fluorescence increase for both CdSe (A) and ZnSe (B) QD (λ_{ex} = 470 nm). Time-resolved photoluminescence decay curves of NBD-liposomes (black) and following a 4 h incubation with QD (red) for CdSe QD(C) and ZnSe QD (D) show a decrease in fluorescence lifetime (λ_{ex} = 470 nm, λ_{em} = 515 nm).

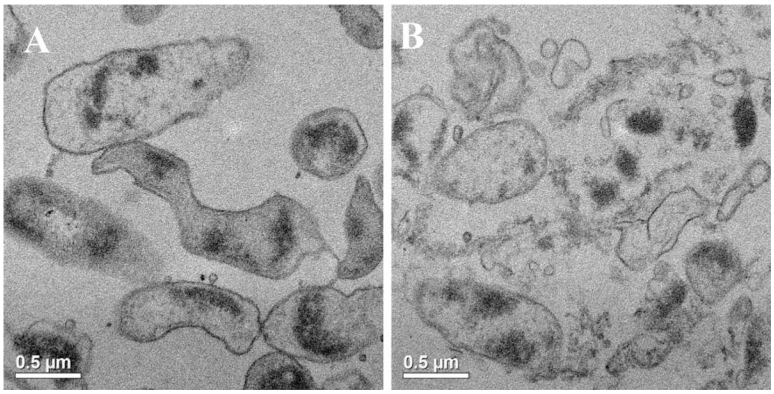

Figure 5.

Representative biological TEM micrographs of *Shewanella oneidensis* MR-1 bacterial cells treated with CdSe/ZnS QD. Image A shows that the interaction of CdSe/ZnS QD with the bacterial cells leads to significant cell malformations. Image B shows significant disintegration of bacterial cells due to interactions with CdSe/ZnS QD.

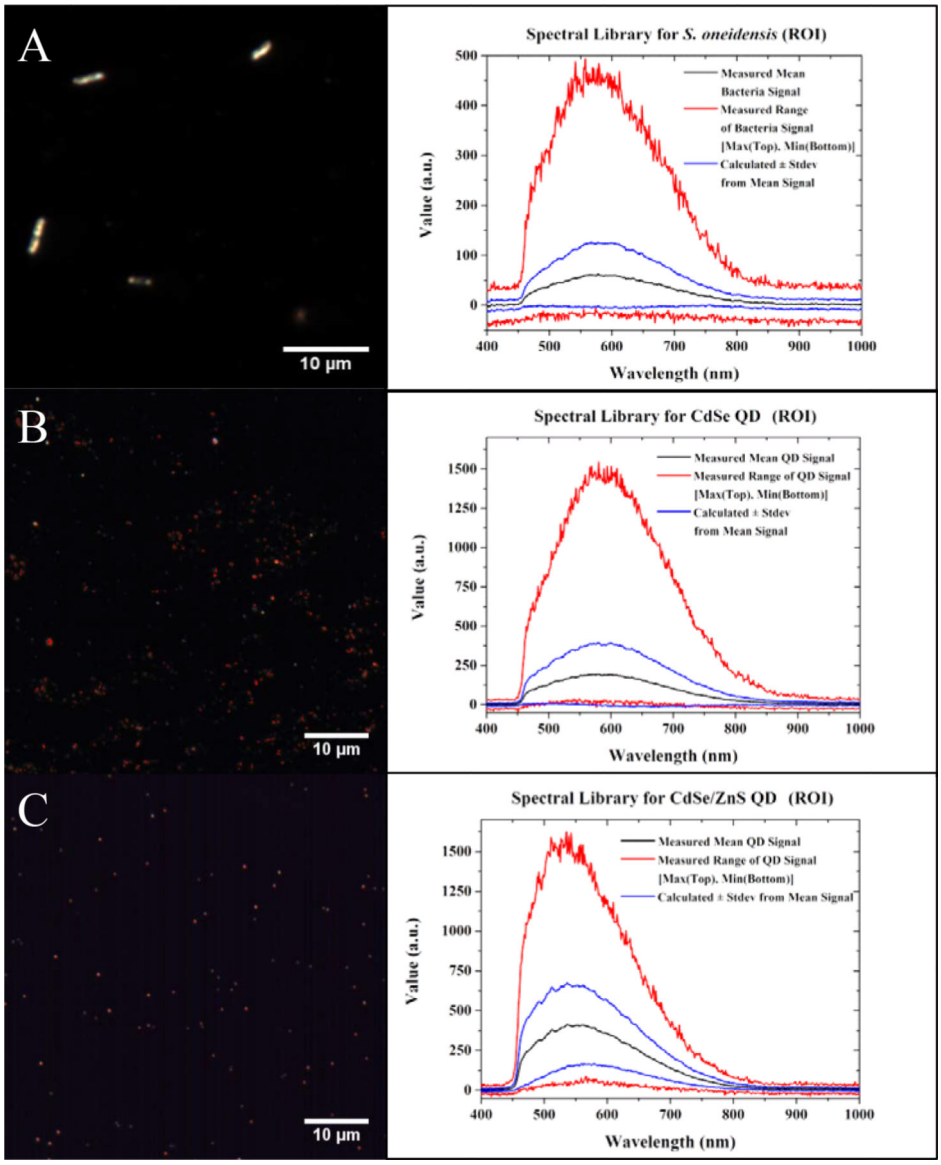

Figure 6.

Hyperspectral reflectance microscopy images of *Shewanella oneidensis* MR-1 ((noted as S.oneidensis in the figure) (A), CdSe QD (B), and CdSe/ZnS (3 ML) QD (C), with the QD false-colored red. The minimum, maximum, and median reflectance spectra for each sample are captured to build a spectral reference library, which is shown to the right of each image. The libraries enable identification of bacterial cells and QD in mixed samples.

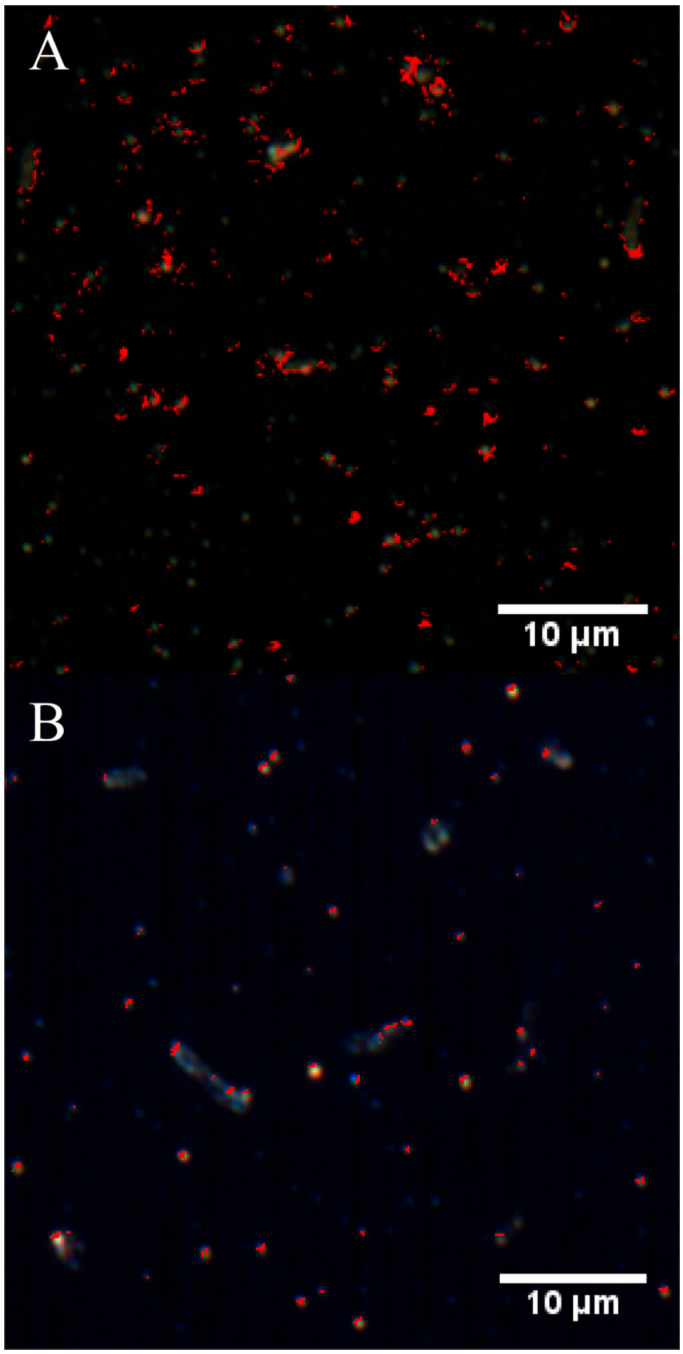

Figure 7.

Images of QD-incubated bacteria samples analyzed using the reference spectral libraries of *Shewanella oneidensis* MR-1 cells (gray) exposed to CdSe QD (A) or CdSe/ZnS (3 ML) QD (B). In both images, pixels displaying the QD spectral signatures are colored red. In many cases, QD are at the vicinity or overlap with bacterial cells, which is indicative of QD membrane association.

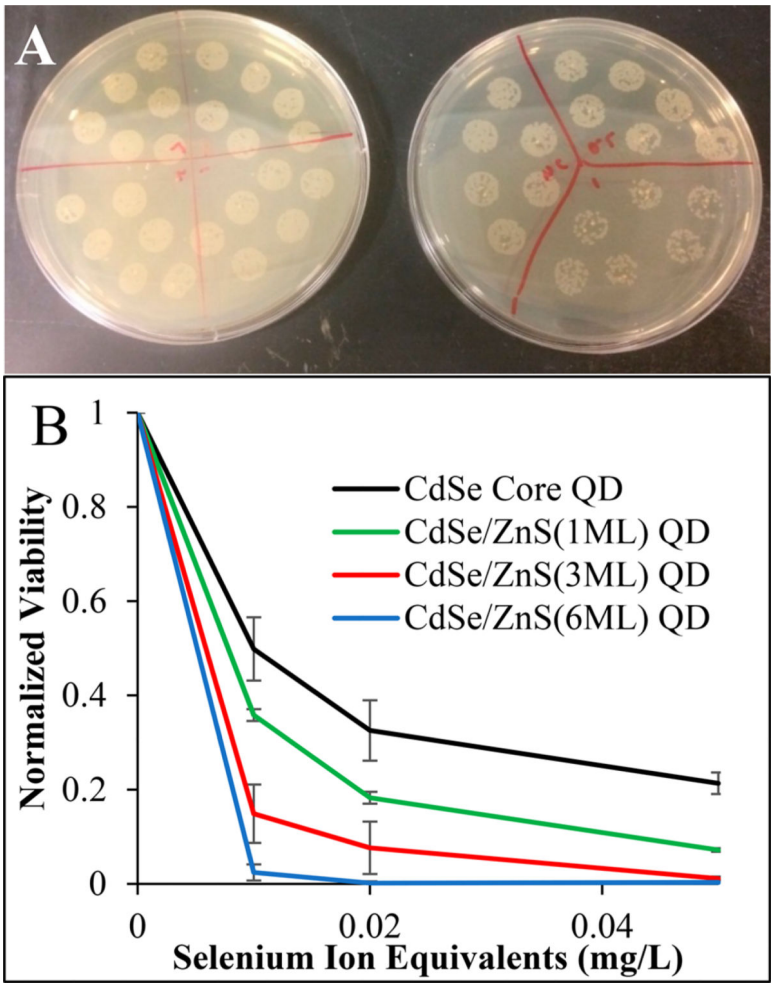

Figure 8.

Shewanella oneidensis MR-1 colony growth after exposure to increasing concentrations of ZnSe QD (left) and CdSe QD (right) compared to negative controls (NC) on each plate (A). Exposing the cells to ZnSe/ZnS QD does not impact cell viability (Figure S6). In contrast, a significant reduction in viability is seen in *Shewanella oneidensis* MR-1 cell viability results following their exposure to CdSe/ZnS QD. A plot of the normalized bacterial cell viability as a function of ZnS shell thickness in CdSe/ZnS QD (B) shows that increasing the QD shell thickness decreases cell viability in a concentration-dependent manner. $N = 4$ biological replicates for each condition, and the error bars represent standard deviation among those replicates.

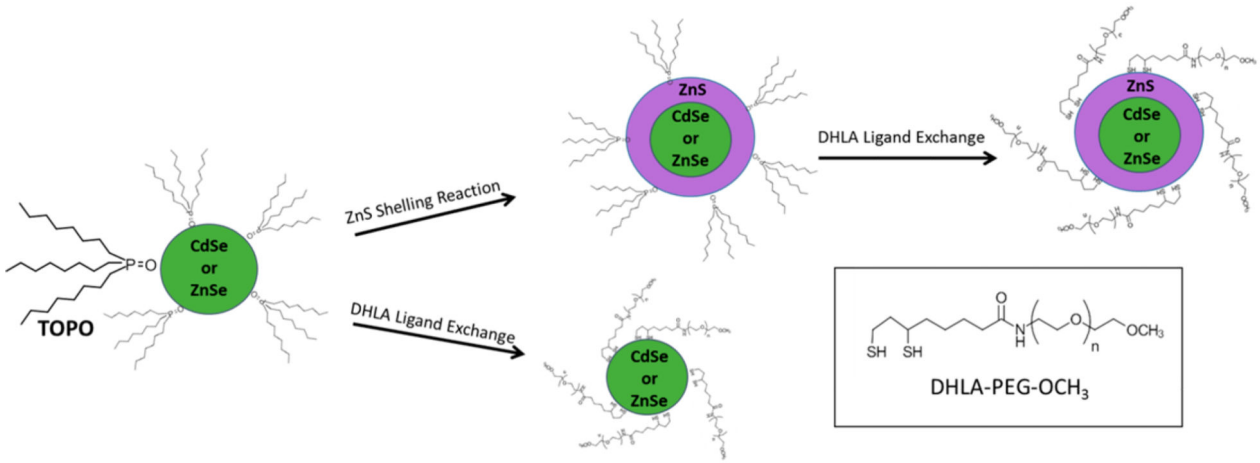

Scheme 1.

Schematic of ZnSe and CdSe QD Shelling to Form ZnSe/ZnS and CdSe/ZnS QD, and Their Ligand Exchange to Enable QD Dispersity in Aqueous Solution by Replacing Hydrophobic TOPO with DHLA-PEG Amphiphilic ligands

Table 1.

Summary of the Fluorescence Lifetime and Exponential Terms Used to Fit the Fluorescence Lifetime Decay Curves for NBD Liposomes Prior to and Following Exposure to CdSe and ZnSe QD[a]

	weighted fluorescence lifetime τ (nsec)	τ_1 (nsec)	A_1 (%)	τ_2 (nsec)	A_2 (%)
NBD- liposomes	5.87 ± 0.23	2.81	54.81	9.58	45.17
CdSe QD and liposomes	5.23 ± 0.02	3.78	72.51	9.24	27.49
ZnSe QD and liposomes	5.17 ± 0.03	3.84	72.48	9.43	27.52

[a]The decrease in fluorescence lifetime and the change from a bi-exponential to a more mono-exponential character of the fluorescence lifetime decay curves are consistent with QD association with the liposome membranes.